Acta of Bioengineering and Biomechanics
Vol. 14, No. 4, 2012

Original paper
DOI: 10.5277/abb120407

A new device for dynamic ventilation-analogue mechanostimulation of pliant tissue layers

KATHARINA GAMERDINGER*, MATTHIAS SCHNEIDER,
EVA SMUDDE, JOSEF GUTTMANN, STEFAN SCHUMANN

Division for Experimental Anesthesiology, University Medical Center Freiburg, Germany.

The experimental mechanostimulation of biological cell and tissue test samples has become a standard method in biomechanics research. In order to apply a static or a dynamic mechanical load on biological tissue a variety of different devices for the mechanostimulation have been developed. While cyclic load applications are typically restricted to sinusoidal or rectangular stimulation patterns, a device for more complex dynamic stimulation patterns which would simulate, for instance, the dynamics during mechanical ventilation does not exist. The dynamic alveolar recruitment/derecruitment has been identified as one of the main causes of ventilator-induced lung injury. Therefore, there is a demand for an experimental ventilation-analogue mechanostimulation of the pulmonary cells and tissue. Here, we present our mechanostimulator combined with a new driving system which is able to produce the ventilation-analogue patterns of a dynamic mechanostimulation. In an experimental setting where the test samples were simulated by silicone-membranes in single-, double- and fourfold membrane configuration, we varied the stimulation amplitude from 5% to 60% surface increase and stimulation frequencies ranging from 15/min to 2000/min. Furthermore, the frequency components of mechanical load applied to the sample at sinusoidal, rectangular and ventilation-analogue mechanostimulations were analyzed by means of a Fast Fourier Transform (FFT). The system allows for a homogeneous mechanostimulation with various temporal profiles which may include frequency components of up to 20 Hz. The relative amount of mechanical load applied to the sample at the main stimulation frequency was 76% during sinusoidal stimulation, 35% during the rectangular stimulation, and 29% to 42% during ventilation analogue stimulation.

Key words: *FFT, mechanostimulation, tissue mechanics*

1. Introduction

Mechanical stimulation is one of the major physiological and environmental influences to which the biological tissue reacts in the living organism. Therefore, one major topic of the current research in biomechanics is related to the influence of the mechanical stimulation of the biological tissue and cells. In *in vitro* experiments a mechanical load is applied to biological tissues and cell-layers to investigate the cell differentiation, cytokine production, cytoskeleton remodelling and other cellular processes [1], [2]. Most mechanostimulators mediate their mechanical load via an uniaxial or biaxial stretch to the sample under test [3], [4]. Typically, these mechanostimulators induce a highly specific mechanical load to the biological test sample.

The devices for an experimental mechanostimulation described in the literature differ with respect to the primary modalities of their mechanical loading condition [5]. Experimental mechanostimulator devices typically allow for the application of a static and a dynamic load. Static mechanical load results in

* Corresponding author: Katharina Gamerdinger, University Medical Center Freiburg, Division for Experimental Anesthesiology, Hugstetter Straße 55, D-79106 Freiburg, Germany. Tel.: +49-761-270-23290, fax: +49-761-270-23280, e-mail: katharina.gamerdinger@uniklinik-freiburg.de

Received: February 14th, 2012
Accepted for publication: September 3rd, 2012

a constant uniaxial or biaxial stretching or compression with a preset elongation. Dynamic mechanical load is typically restricted to a sinusoidal or rectangular profile with a preset frequency (table 1). However, dynamic mechanostimulations which occur in the living organism, e.g., the ones associated with the cardiovascular or respiratory system, are characterized by cyclic load profiles which are by far more complex than a sinusoidal or rectangular pattern.

With respect to mechanical ventilation it is generally accepted that the cyclic alveolar recruitment/derecruitment, which is associated with considerable mechanical shear stress in the alveolar parenchyma, is one of the major causes of ventilator-induced lung injury (VILI) [6]. The cyclic alveolar recruitment/derecruitment and hence VILI is associated with a temporal ventilatory pattern that is considerably influenced by the lung mechanics. The lung mechanics affect, for instance, the dynamics of the expiration. The time-constant for the passive expiration is defined by the compliance and resistance of the respiratory system and the artificial airways [7]. To investigate the effects of the ventilation dynamics on the isolated pulmonary cells or tissue, a simulation of these dynamics with an experimental mechanostimulator device is required.

Here, we present a new system combining a mechanostimulator with a linear motor drive which allows the simulation of complex dynamic profiles of mechanical load. The purpose of the study was to test the system under a variety of dynamic mechanostimulation patterns (i.e., sinusoidal, rectangular and ventilation-analogue) and to analyze the frequency components of these patterns quantitatively using a Fast Fourier Transform. We used self-made polydimethylsiloxane (PDMS) membranes as test samples instead of soft biological tissue which shows unknown variances in its mechanical characteristics. The test samples were deflected with sinusoidal, rectangular and ventilation-analogue stimulation patterns and the resulting stress-strain profiles were analyzed in terms of amplitude and frequency components.

2. Materials and methods

2.1. Mechanostimulator

We used a mechanostimulator, developed by our group, for the mechanostimulation and measurement of the counterpressure resulting from the sample's response to mechanical load [8], [9]. The mechanostimulator served as an environment for the cultivation and mechanostimulation of flat biological tissue samples like cellular monolayers or thin tissue slices, e.g., precision cut lung slices [10] or isolated diaphragms of small animals [11]. It consists of two chambers which are separated by a highly flexible impermeable silicone membrane. The sample is placed on this membrane either circumferentially fixed by clamping in the case of tissue, e.g., precision cut lung slices [10] or diaphragms [11], or directly adhered to the surface of the PDMS membrane, in the case of cells. On one side, the lower chamber, or pressure chamber, is connected to a piston pump whose position is controlled by a linear motor (figure 1). On the other side the pressure chamber is attached to a pressure measuring device. The upper chamber serves as a supply chamber to provide nutrition to the tissue sample under test.

In the mechanostimulator, a biaxial load is exerted by applying the bubble inflation technique [12]. Therefore, a defined fluid volume is displaced into the pressure chamber below the sample. The pressure inside this chamber results from the sample counterforce against deformation and thus represents the mechanical stress of the tissue sample. By measuring the pressure and the tissue-deforming volume, the secant modulus of the sample during the deflection can be determined [8].

2.2. Membranes

When investigating biological tissue samples an air tight sealing between the pressurized space below the tissue (pressure chamber) and the space above (supply chamber) is achieved by placing the sample of interest on top of an air tight membrane. In order to achieve the lowest possible impact of the membrane counterforce on the generated pressure we use self-fabricated membranes [9] that consist of polydimethylsiloxan (PDMS, Sylgard® 184, Dow Corning, Michigan, USA).

The PDMS-membranes possess linear mechanical characteristics [9] and are therefore clearly more suitable for our purposes than biological test samples which show unknown variances in their mechanical behaviour. The membranes were produced as described by ARMBRUSTER et al. [9]. In brief, base resin and curing agent were mixed with a weight ratio of 10:1. The mixture was placed on a wafer-chuck and the membranes were produced in a spin-coating process.

The rotation speed was 600 rpm and rotation time was 1 min. After the spin-coating the membranes were polymerized for at least 4 h at 68 °C. By this procedure membranes of a diameter of 22 mm and a thickness of 80 μm with a secant modulus of 1.9 MPa were obtained [9].

2.3. Finite Element Simulation

A finite element simulation (FES) was carried out using dedicated software (COMSOL Multiphysics 4.0, COMSOL Multiphysics, Göttingen, Germany). Based on a linear elastic model with 11976 tetrahedral elements, the deflection of a flat tissue of 80 μm thickness, 11 mm radius and Young's modulus of 1.9 MPa (i.e., the characteristics of a PDMS membrane) inside the mechanostimulator was simulated for the application of a maximal pressure of 20 mbar. From the calculated values of subsequent simulation steps the relationships between pressure, volume and von-Mise-stress were derived.

2.4. Drive for mechanostimulation

A drive system for the mechanostimulation was constructed to apply an identical mechanostimulation pattern to four test samples within separate mechanostimulators at the same time. For that purpose, a computer controlled linear motor system (PS01-23S × 80, LinMot, Spreitenbach, Switzerland) was connected to four piston pumps (figure 1a, 1c), each operating separately one mechanostimulator. This way we ensured that possible compliance discrepancies between samples would not lead to a diverse distribution of stimulation volume as it could be the case if the four mechanostimulators were driven by one pump. A self developed software based on LabView (version 7.1, National Instruments Corp., Austin, TX) controlled the movement of the linear motor.

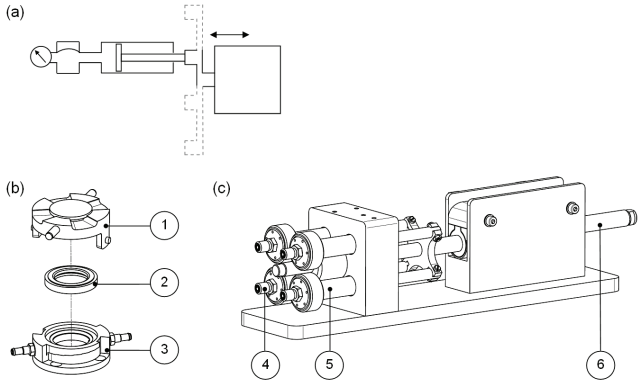

Fig. 1. (a) Schematic drawing of a single mechanostimulator connected to a pressure box on one side and to the drive-system via a piston pump on the other. For the simultaneous activation of four mechanostimulators, each is connected to a separate piston pump and the four piston pumps are connected to one linear motor. The pressure resulting from the deflection of the test sample is measured by a pressure sensor. (b) Schematic of the mechanostimulator, 1: upper chamber with a glass lid, 2: membrane holder, 3: lower chamber with tube connectors. (c) Schematic of the drive system, 4: tube connector, 5: piston pump, 6: armature of the linear motor

The accuracy of the measurement of the pressure–volume relationship inside the pressure chamber critically depends on the amount of compressible gas inside the pressurized system. In order to keep the volume constant, the amount of compressible gas needs to be reduced. To this end, hydraulic-pneumatic coupling was integrated in the driving system by partly replacing the compressible air with incompressible water. Only a small volume of 4 mL below the membrane remained air-filled.

2.5. Test measurements

The PDMS-membranes serving as substitutes for biological tissue samples were placed inside the mechanostimulator either in single-, double- or in four-fold membrane configuration. The manifold membrane configurations simulate the measurement of test-samples (PDMS-membranes on top), placed on the carrier membrane (lowest PDMS-membrane).

Four different patterns of mechanostimulation were applied, (i) sinusoidal, (ii) rectangular, (iii) ventilation-analogue representing the stimulation profile of a mechanically ventilated healthy lung, and (iv) ventilation-analogue representing the stimulation profile of a mechanically ventilated lung with Acute Respiratory Distress Syndrome (ARDS).

2.6. Dynamics of mechanostimulation

In order to investigate the dynamic range of the mechanostimulator system we performed experiments using a cyclic mechanostimulation at repetition rates ranging from 15/min to 2000/min, which includes the frequency of fast human breathing up to the highest frequency components of the breathing signal of a mouse. The performance of the system has been tested at amplitude volumes of 0.5, 1 and 2 mL, corresponding to a surface increase of 5%, 20% and 60%, respectively (see Appendix). The linear motor's movement was determined by measuring the voltage across a linear

potentiometer (CIPGST258M220KA, Radioohm, Bad Homburg, Germany) whose slider was connected to the armature of the motor. The pressure inside each mechanostimulator pressure chamber was measured using a piezoresistive pressure transducer (SI – special instruments GmbH, Nördlingen, Germany). The sampling frequency was set to 500 1/s.

The effects of the mechanical impedance of the sample on the dynamics of the pressure development were analyzed by performing a sinusoidal cyclic mechanostimulation. As a measure for the mechanical impedance of the sample configuration we defined the elastance $E_{1\,mL}$ as the quotient of pressure and volume at a deflection with 1mL applied volume. In this experiment, stimulation with a typical amplitude of 1 mL volume at a frequency of 15/min was chosen.

First, four single membranes were tested separately. Each membrane was placed inside one of four mechanostimulators which were connected in parallel (single-membrane configuration). This procedure was repeated with two membranes (one placed upon the other) with the mechanostimulator (double-membrane configuration) and with four membranes placed within each mechanostimulator (fourfold-membrane configuration). Thereby the single-membrane configuration corresponds to the minimal mechanical impedance of the mechanostimulator, i.e., without sample tissue and the fourfold-membrane configuration corresponds to a high mechanical impedance, reflecting the mechanostimulation of tendon tissue of about 2.5 mm thickness [13]. All configurations were deflected conjointly with the same stimulation pattern.

2.7. Stimulation profiles

To analyze the frequency components of the cyclic mechanical load which is transferred to the test sample the mechanostimulator was driven with sinusoidal, rectangular and ventilation-analogue profiles simulating the ventilatory pattern which is associated with the volume controlled ventilation. Again an amplitude of 1 mL volume and a frequency of 15/min were chosen. In order to simulate moderate mechanical impedance the double-membrane configuration was chosen.

2.8. Ventilation-analogue profiles

The ventilation-analogue mechanostimulation was realized with two different stimulation patterns to simulate different dynamic conditions: firstly, mimicking the expiratory profile of the healthy lung, i.e., with an expiratory time-constant of 400 ms, and secondly, mimicking the expiratory profile of ARDS, i.e., with a short expiratory time-constant of 133 ms [7].

2.9. Frequency analysis

To analyze the frequency components of the mechanical load applied to the sample, the frequency spectrum of the pressure profile which resulted from the mechanostimulation was calculated using the Fast Fourier Transform. To compare the amounts of mechanical load transferred to the sample in and above the main stimulation frequency we calculated the sums of amplitudes of the normalized frequency spectrum within the frequency (f) ranges 0.1 Hz $< f <$ 0.4 Hz and 0.1 Hz $< f <$ 10 Hz. The resulting values were divided by each other resulting in the energy distribution index (EDI). An EDI of 1 would mean that 100% of the total energy transferred to the sample is transferred at the stimulation frequency.

3. Results

3.1. Finite element simulation

The finite element stimulation of a tissue inside the mechanostimulator revealed nonlinear relationships between volume, pressure and von-Mise-stress and a linear relationship between von-Mise-stress and relative increase in surface area (figure 2a). The von-Mise-stress was distributed homogeneously across the deflected tissue (figure 2b).

3.2. Dynamics of the drive system

Using the mechanostimulator in combination with the linear motor drive system we were able to apply different mechanical load profiles. The drive system allowed us to vary the amplitude from 0 to 2.8 mL volume (reflecting an increase in the surface of the sample of up to 100%, data not shown). At an amplitude of 0.5 mL we were able to apply up to 1200, at amplitudes of 1.0 mL and 2.0 mL we could apply up to 600 sinusoidal deflections per minute (figure 3).

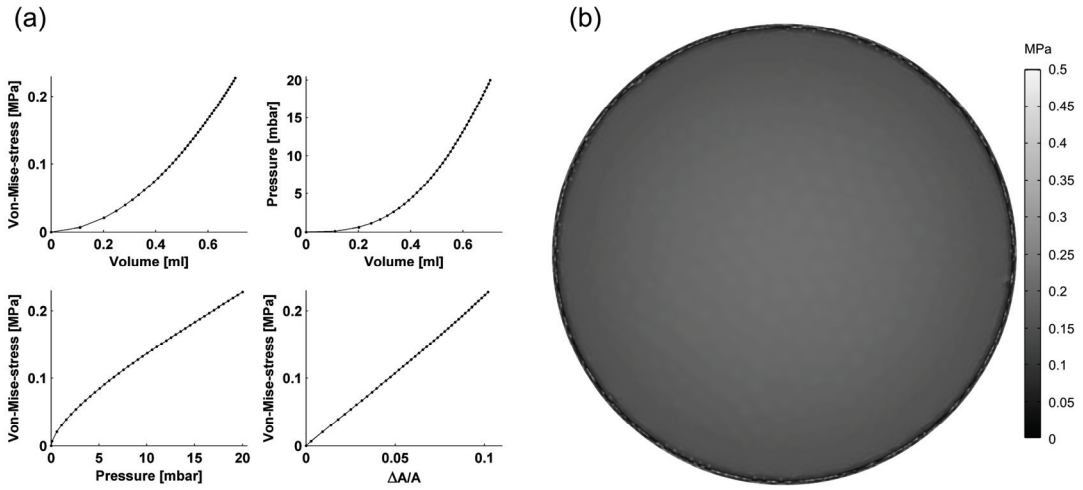

Fig. 2. Analysis of volume, pressure, von-Mise-stress and strain in a tissue deflected inside the mechanostimulator. Membrane deflection was simulated for the application of a maximal pressure of 20 mbar in finite element simulation utilizing a linear elastic model with 11976 tetrahedral elements. (a) Relationships of volume, pressure, average von-Mise-stress across the membrane and strain in terms of relative area increase (ΔA/A). (b) Distribution of the von-Mise-stress across the membrane. The von-Mise-stress was found to be almost constantly distributed across the membrane. The inhomogeneities along the circumferential border of the membrane result from calculation artefacts reasoned by the limited number of boundary points

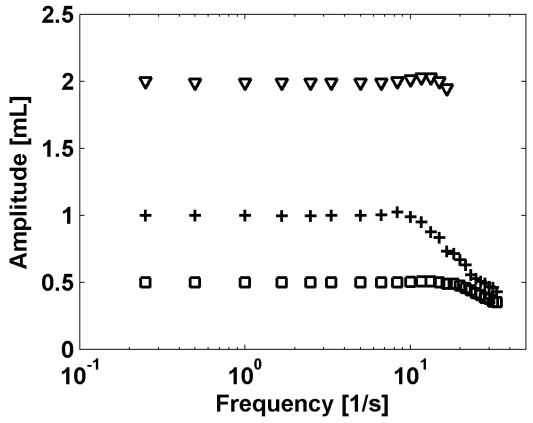

Fig. 3. Volume displacement amplitudes achieved at different frequencies of sinusoidal stimulation profiles. The set amplitudes were 2 mL (∇), 1 mL (+) and 0.5 mL (□)

3.3. Influence of mechanical sample impedance

Close inspection of the pressure curves revealed that sinusoidal volume application resulted in a sinusoidal pressure profile with flattened slopes in the low pressure-volume range. The impedance of the sample increased with the number of membranes within each mechanostimulator (single-membrane configuration $E_{1\,mL}$ = 28.3 mbar/ml, double membrane configuration: $E_{1\,mL}$ = 50.0 mbar/ml, four membrane configuration: $E_{1\,mL}$ = 73.5 mbar/ml). This was reflected by the maximal pressure increasing from 28.3 to 73.5 mbar with the number of membranes increasing from 1 to 4 (figure 4). There were no differences detectable in the applied volume amplitudes when we tested single- or double- or four-membrane configuration with 15 sinusoidal deflections per minute and a targeted volume application of 1 mL (figure 4). Furthermore the normalized frequency components of the measured pressure signal were identical in all three membrane configurations (lower panels figure 4b). The frequency spectra of the pressure curves following the sinusoidal mechanostimulation showed one main frequency component at 0.25 Hz and one side frequency component at 0.45 Hz (lower panels of figure 4). The main frequency was normalized and set to 1, related to this the side frequency amplitude was 0.36. Both were independent of the mechanical impedance of the sample. We did not observe relevant time shifts between volume and pressure signals.

3.4. Rectangular and ventilation-analogue stimulation profiles

We were able to apply the rectangular and the ventilation-analogue load patterns to the mechanostimulator in double-membrane configuration (upper panels of figure 5). A close inspection of the pressure curves revealed that during rectangular volume application the initial rapid pressure increase ended in a pressure peak with subsequent exponential relaxation decay until a pressure plateau was reached. During ventilation-analogue volume application the pres-

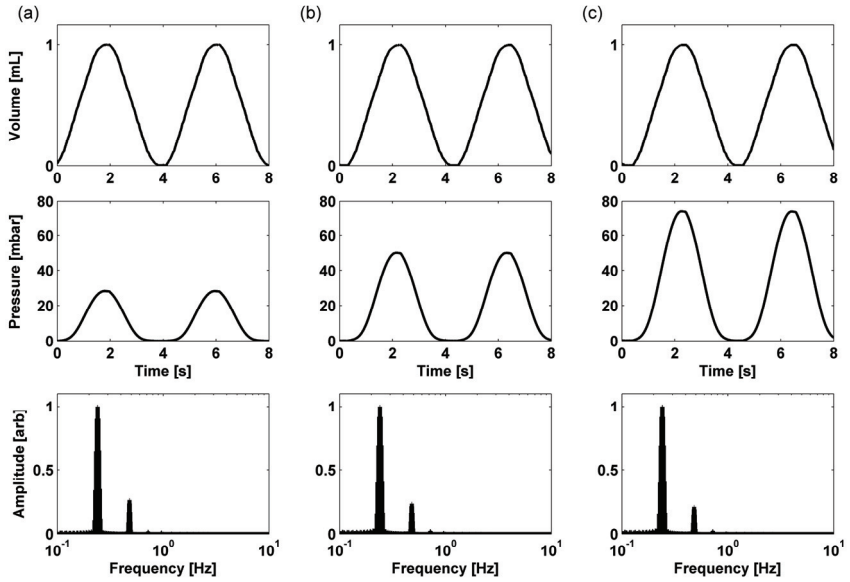

Fig. 4. Frequency analysis of the sinusoidal pattern of the mechanostimulation using a single-membrane, a double-membrane and a fourfold-membrane configuration. (a) Average of 4 single membranes. (b) Average of 4 double membranes. (c) Average of 4 fourfold membranes. Top: insufflated volume over time. Middle: pressure data concerning the applied volume. Bottom: frequency components of the pressure signal according to Fast Fourier Transform. Frequencies are normalized to the main frequency of the stimulation; off-set components are not shown

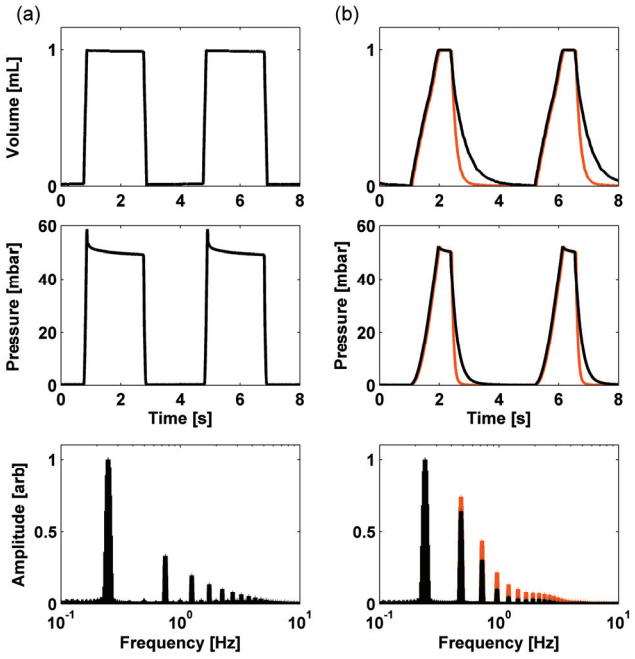

Fig. 5. Volume and pressure data over time and frequency components of the pressure signal in a double-membrane configuration with (a) a rectangular deflection profile and (b) volume and pressure curves and respective frequency spectra resulting from the ventilation-analogue profile simulating the healthy lung (black) and an ARDS lung (red). Top: insufflated volume over time. Middle: pressure data concerning the applied volume. Bottom: frequency components of the pressure signal according to Fast Fourier Transform. Frequencies are normalized to the main frequency of the stimulation; off-set components are not shown

sure increase showed a reduced pressure rise in the low pressure-volume range followed by a nearly linear increase, ending in a small peak with a small relaxation decay. During the volume decays simulating expiration of a healthy and an ARDS lung pressure followed an exponential curve similar to the respective volume curves with a steeper slope in the low pressure–volume range. The frequency spectra of the pressure curve revealed side frequencies of up to 10 Hz for the rectangular mechanostimulation profile.

When we applied the ventilation-analogue stimulation profiles, the frequency spectrum showed frequency components of up to about 8 Hz (the lower panel of figure 5b). Higher frequency components were more pronounced for the profile that mimicked the mechanostimulation of injured lungs (figure 5b, red line) compared to the one that simulated the mechanostimulation of healthy lungs (figure 5, black line). The energy distribution index differed markedly between stimulation profiles: sinusoidal EDI = 0.76, rectangular EDI = 0.35, ventilation-analogue mimicking healthy lungs EDI = 0.41 and ventilation-analogue mimicking injured lungs EDI = 0.29.

4. Discussion

In this “proof of concept”-study we investigated the dynamic behaviour of our improved device for the

mechanostimulation of biological tissue samples. The main findings of our study can be summarized as follows: (a) the mechanostimulator allows for the application of a mechanical load that leads to an increase in the surface of the analyzed samples of up to 100%; (b) The von-Mise-stress evoked inside the sample is distributed very homogeneously; (c) the cyclic mechanical stimulation can be applied at repetition rates ranging from zero (static condition) up to 1200 sinusoidal deflections per minute for volume applications of 0.5 mL; (d) our device allows for the application of mechanostimulations with arbitrary temporal profiles including frequency components of up to 20 Hz and (e) in comparison to a sinusoidal profile the ventilation-analogue mechanostimulation is characterized by a noteworthy content of high frequency components which depends, for instance, on the time-constant of passive expiration.

To the best of our knowledge, we present the first device that allows a cyclic mechanostimulation with variable temporal profiles. Furthermore, by measuring the pressure resulting from the counterforce of the sample against deformation we can reliably determine the counterforce of the tissue under test resulting from its deflection as response to the applied mechanical load. Thus, we can determine the stress–strain relationship of the sample under test, i.e., its mechanical characteristics [8]. For an easy use one could produce a series of reference membranes with a given Young's modulus and collect experimental data related to the pressure–volume relationship development for the system consisting of the base membrane and of the reference membrane. The pressure–volume relationship of a tissue sample could be measured and Young's modulus could be determined by comparison to the reference data and accounting for the sample thickness in comparison with the thickness of the reference sample.

4.1. Simulating in situ mechanostimulation

Mechanostimulations are a ubiquitous phenomenon in the living organism. Most cells and tissues experience static and/or dynamic mechanical load caused by tensile or compressive strain under physiological conditions. The mechanical behaviour of most living tissues is nonlinear and frequency dependent. In this study we focussed on the dynamics of the mechanostimulation that characterize the mechanical ventilation of the lung.

During spontaneous breathing the mechanical load on the pulmonary tissue is akin to a sinusoidal profile. In contrast, during mechanical ventilation the stimulation profile of the lung tissue differs considerably from a sinusoidal pattern. In this context, it has to be noted that the amplitude of the mechanical load spectrum at a certain frequency is a measure for the energy transferred to the sample at this frequency, and it is obvious that the high frequency components are related to the transfer of high energy which implies an increased risk of pulmonary tissue damage compared to the lower frequency components of the same amplitude.

We have applied sinusoidal, rectangular and ventilation-analogue mechanostimulation profiles with similar amplitudes in the time domain. The frequency analysis has shown that these signals differ in their content of high frequency components. In other words, the difference between these stimulation profiles lies in the amount of energy transferred to the sample at the frequency components above the main stimulation rate. With this in mind it is obvious that by stimulation at the same amplitude with a sinusoidal profile least energy is transferred to the sample. The energy transferred to the sample by ventilation-analogue profiles lies closer to the rectangular than to the sinusoidal profile (the latter even more distinct for the "ARDS" profile compared to the "healthy lung" profile).

Table 1. Published devices for application of mechanical stimulation of biological tissue samples

Authors	Stretch apparatus	Stimulus waveform
BANES et al. 1985 [14]	Flexercell	on/off (rectangular
TSCHUMPERLIN et al. 1998 [4]	Cell-stretching device	on/off (rectangular)
PUGIN et al. 1998 [15]	"Plastic lung"	sinusoidal
TRZEWIK et al. 2004 [16]	Cell drum	resonance oscillation sinusoidal
AROLD et al. 2007 [17]	Stretching apparatus	sinusoidal
GERSTMAIR et al. 2009 [18]	Computer-controlled stretch device	on/off (rectangular)
WANG et al. 2009 [19]	Flexercell	on/off (rectangular)
LUJAN et al. 2011 [3]	Bioreactor	sinusoidal

Most devices for the mechanostimulation of biological tissue described in the literature allow for the application of a sinusoidal or rectangular temporal profile (table 1). However, in order to investigate the influence of the frequency components of a stimulation profile on the biological response of a sample, i.e., tissue integrity,

viability, inflammation and/or mechanical properties of tissue probes, the option for applying multiple stimulation profiles, e.g., sinusoidal, rectangular or ventilation-analogue profiles, is required.

Focusing on the mechanostimulation of the lungs we have to differentiate between two situations: 1) the lungs during spontaneous breathing and 2) the lungs during mechanical ventilation. During spontaneous breathing the lungs are breathwise loaded with a temporal profile similar to a sinusoidal pattern. During mechanical ventilation the intrapulmonary pressure course, e.g., during volume controlled ventilation, reveals a linear increase during inspiration, an abrupt release when inspiration switches to expiration and an exponential decay curve during expiration. Thus, the temporal stress profile of the lungs under mechanical ventilation contains considerably more high frequency components compared to the profile during spontaneous breathing, as we demonstrated in our analysis. Compared to the healthy lung the injured lung is characterized by a considerably reduced volume distensibility which results in a shorter time-constant of passive expiration. Thus the injured lung is exposed to a load profile with components of higher frequencies than the healthy lung that is ventilated under the same conditions. This was also shown by the energy distribution index. During sinusoidal mechanostimulation 76% of the total mechanical load transferred to the sample is transferred at the desired frequency range. In contrast, with rectangular and ventilation analogue mechanostimulation only 30 to 42% of the energy transferred to the sample at the chosen frequency range. It has to be noted that an ideal sinusoidal stimulation profile (EDI = 1) would transfer the energy only in the set frequency range. In other words, by mechanostimulation with a ventilation-analogue profile the total energy transfer to the sample is two to three times higher compared to an ideal sinusoidal stimulation at the same amplitude. As a consequence, the sinusoidal profile is inadequate to describe the mechanostimulation of the lungs parenchyma during mechanical ventilation. To understand the mechanisms which lead to a ventilator-induced lung injury the experimental biomechanics research requires devices which allow for the in vitro application of a cyclic mechanostimulation with variable frequency components of pressure profiles. With this study we claim to have developed an approach for this task.

4.2. Limitations of the study

We substituted biological tissue by pliant membranes of PDMS. Using this substitute material we were able to perform our measurements with samples of similar material properties which remain constant over time. When determining the characteristics of a new device this is preferable compared to the use of biological material with comparable high variance and uncertain temporal behaviour in its material properties. With this material we did not observe any relevant time shift between the volume displacement and the pressure signal, which might occur in biological tissue. However, such analysis could be made with our system and would be helpful in determining viscoelastic properties of the sample tested.

We only investigated three types of stimulation profiles: a sinusoidal, a rectangular and a ventilation-analogue profile. Other profiles could be realized with our drive, e.g., a positive end expiratory pressure could be simulated by a shift of the drive's offset position resulting in a constant deflection component. Moreover, other cyclic stimulation profiles being composed of frequency components up to 20 Hz, e.g., the mechanostimulation of the arterial wall or the temporal profile of the blood pressure could be realized accordingly. However, this lies beyond the scope of this study which was aimed to proof the principle of a 'realistic' mechanostimulation with patterns related to the mechanical ventilation.

4.3. Thermodynamics

A rapid gas compression is always associated with an increase in temperature. For the rectangular stimulation profile this resulted in increased peak pressure amplitudes followed by a relaxation course (figure 5). For the ventilation-analogue stimulation this effect was less pronounced due to the slower rise of the applied load. Such effects were also described earlier for a similar mechanostimulator environment [8]. It has to be noted that in the case of mechanical ventilation similar effects should take place in the lung. Furthermore, the pressure–volume ralationship is nonlinear (figure 2) resulting in deviations between the applied volume and the resulting pressure profiles (figures 4 and 5). However, if required, such effects could be compensated for by respective customization of the stimulation curve.

5. Conclusion

A realistic simulation of mechanical load on biological tissue requires the application of a temporal load profile analogue to the profile the tissue would

experience in situ. We have developed a system to realize such profiles. Our mechanostimulator allows for a load application that leads to an increase in the surface of the analyzed samples of up to 100% and for the application of mechanostimulation with arbitrary temporal profiles including frequency components of up to 20 Hz. Thereby the mechanical stress inside the tissue is distributed very homogeneously. In comparison to a sinusoidal profile the ventilation-analogue mechanostimulation is characterized by a noteworthy content of high frequency components which depends, for instance, on the time-constant of passive expiration. With our new system we are able to configure the frequency components of the profile of the applied mechanical load and furthermore to identify the frequency components of the stress resulting in the tissue.

Acknowledgements

The authors would like to thank Sarah Buehler, Ph.D., and Michael Bergmann for the careful revision of the manuscript and David Schwenninger, Ph.D., for performing the finite element simulation. This work was supported in parts by the German Research Foundation DFG (Deutsche Forschungsgemeinschaft); contract grant number: DFG GU 561/4-2.

References

[1] EDWARDS Y.S., *Stretch stimulation: its effects on alveolar type II cell function in the lung*, Comp. Biochem. Physiol. A Mol. Integr. Physiol., 2001, 129, 245–260.

[2] FOSTER C.D., VARGHESE L.S., GONZALES L.W., MARGULIES S.S., GUTTENTAG S.H., *The Rho pathway mediates transition to an alveolar type I cell phenotype during static stretch of alveolar type II cells*, Pediatr. Res., 2010, 67, 585–590.

[3] LUJAN T.J., WIRTZ K.M., BAHNEY C.S., MADEY S.M., JOHNSTONE B., BOTTLANG M., *A novel bioreactor for the dynamic stimulation and mechanical evaluation of multiple tissue-engineered constructs*, Tissue Eng. Part C Methods, 2011, 17, 367–374.

[4] TSCHUMPERLIN D.J., MARGULIES S.S., *Equibiaxial deformation-induced injury of alveolar epithelial cells in vitro*, Am. J. Physiol., 1998, 275, L1173–1183.

[5] LAKSHMANAN V., YANG T.H., REUBEN R.L., HAMMER J., ELSE R.W., *Multi-scale techniques of measuring the dynamic properties of biological tissues*, Technol. Health Care, 2006, 14, 297–309.

[6] GATTINONI L., PROTTI A., CAIRONI P., CARLESSO E., *Ventilator-induced lung injury: the anatomical and physiological framework*, Crit. Care Med., 2010, 38, S539–548.

[7] GUTTMANN J., EBERHARD L., FABRY B., BERTSCHMANN W., ZERAVIK J., ADOLPH M., ECKART J., WOLFF G., *Time constant/volume relationship of passive expiration in mechanically ventilated ARDS patients*, Eur. Respir. J., 1995, 8, 114–120.

[8] SCHUMANN S., STAHL C.A., MOLLER K., SCHNEIDER M., METZKE R., WALL W.A., PRIEBE H.J., GUTTMANN J., *Contact-free determination of material characteristics using a newly developed pressure-operated strain-applying bioreactor*, J. Biomed. Mater Res. B Appl. Biomater., 2008, 86B, 483–492.

[9] ARMBRUSTER C., SCHNEIDER M., SCHUMANN S., GAMERDINGER K., CUEVAS M., RAUSCH S., BAAKEN G., GUTTMANN J., *Characteristics of highly flexible PDMS membranes for long-term mechanostimulation of biological tissue*, J. Biomed. Mater Res. B Appl. Biomater., 2009, 91, 700–705.

[10] DASSOW C. et al., *Biaxial distension of precision-cut lung slices*, J. Appl. Physiol., 2010, 108, 713–721.

[11] ARMBRUSTER C., DASSOW C., GAMERDINGER K., SCHNEIDER M., SUMKAUSKAITE M., GUTTMANN J., SCHUMANN S., *Mechanostimulation, electrostimulation and force measurement in an in vitro model of the isolated rat diaphragm*, Physiol. Meas., 2011, 32, 1899–1912.

[12] SELBY J.C., SHANNON M.A., *Apparatus for measuring the finite load-deformation behavior of a sheet of epithelial cells cultured on a mesoscopic freestanding elastomer membrane*, Rev. Sci. Instrum., 2007, 78, 094301.

[13] WREN T.A.L., LINDSEY D.P., BEAUPRÉ G.S., CARTER D.R., *Effects of Creep and Cyclic Loading on the Mechanical Properties and Failure of Human Achilles Tendons*, Ann. Biomed. Eng., 2003, 31, 710–717.

[14] BANES A.J., LINK G.W., SNYDER L.R., *Comparison of reversed-phase columns for the separation of tryptic peptides by gradient elution. Correlation of experimental results and model prediction*, J. Chromatogr., 1985, 326, 419–431.

[15] PUGIN J., DUNN I., JOLLIET P., TASSAUX D., MAGNENAT J.L., NICOD L.P., CHEVROLET J.C., *Activation of human macrophages by mechanical ventilation in vitro*, Am. J. Physiol., 1998, 275, L1040–1050.

[16] TRZEWIK J., ARTMANN-TEMIZ A., LINDER P.T., DEMIRCI T., DIGEL I., ARTMANN G.M., *Evaluation of lateral mechanical tension in thin-film tissue constructs*, Ann. Biomed. Eng., 2004, 32, 1243–1251.

[17] AROLD S.P., WONG J.Y., SUKI B., *Design of a new stretching apparatus and the effects of cyclic strain and substratum on mouse lung epithelial-12 cells*, Ann. Biomed. Eng., 2007, 35, 1156–1164.

[18] GERSTMAIR A., FOIS G., INNERBICHLER S., DIETL P., FELDER E., *A device for simultaneous live cell imaging during uniaxial mechanical strain or compression*, J. Appl. Physiol., 2009, 107, 613–620.

[19] WANG Y., MACIEJEWSKI B.S., SOTO-REYES D., LEE H.S., WARBURTON D., SANCHEZ-ESTEBAN J., *Mechanical stretch promotes fetal type II epithelial cell differentiation via shedding of HB-EGF and TGF-alpha*, J. Physiol., 2009, 587, 1739–1753.

Appendix

The relation between volume and surface area of the membrane is defined by the geometry of a spherical cap [11].

The surface increase through volume application can be calculated as follows.

The surface of a spherical cap A is described by

$$A = \pi(R^2 + h^2) \tag{A1}$$

where R is the radius of the basic circle of the cap and h is the height of the cap.

The volume V of the spherical cap is defined by

$$V = \frac{\pi}{2} R^2 h - \frac{\pi}{2} h^3 . \tag{A2}$$

Using both equations we can eliminate R:

$$A = 2\frac{V}{h} - \frac{2}{3}\pi h^2 . \tag{A3}$$

To allow the calculation of surface area without measurement of h, equation (A2) can be solved for h by using Cardano's method for cubic equations:

$$h = \sqrt[3]{\frac{3V}{\pi} + \sqrt{\left(\sqrt{\frac{3V}{\pi}}\right)^2 + R^6}} + \sqrt[3]{\frac{3V}{\pi} + \sqrt{\left(\sqrt{\frac{3V}{\pi}}\right)^2 + R^6}} . \tag{A4}$$